STEM CELLS TRANSLATIONAL MEDICINE®

FETAL AND NEONATAL STEM CELLS

Bioprinted Amniotic Fluid-Derived Stem Cells Accelerate Healing of Large Skin Wounds

ALEKSANDER SKARDAL,[a]* DAVID MACK,[a]* EDI KAPETANOVIC,[b] ANTHONY ATALA,[a] JOHN D. JACKSON,[a] JAMES YOO,[a] SHAY SOKER[a]

Key Words. Fetal stem cells • Angiogenesis • Cellular therapy • Mesenchymal stem cells • Skin grafts

[a]Wake Forest Institute for Regenerative Medicine, Winston-Salem, North Carolina, USA; [b]Cornell University, Ithaca, New York, USA

*Contributed equally as first authors.

Correspondence: Shay Soker, Ph.D., Wake Forest Institute for Regenerative Medicine, Winston-Salem, North Carolina 27157, USA. Telephone: 336-713-7295; Fax: 336-713-7290; E-Mail: ssoker@wakehealth.edu

Received July 16, 2012; accepted for publication September 17, 2012; first published online in SCTM *EXPRESS* October 29, 2012.

1066-5099/2012/$20.00/0

http://dx.doi.org/10.5966/sctm.2012-0088

ABSTRACT

Stem cells obtained from amniotic fluid show high proliferative capacity in culture and multilineage differentiation potential. Because of the lack of significant immunogenicity and the ability of the amniotic fluid-derived stem (AFS) cells to modulate the inflammatory response, we investigated whether they could augment wound healing in a mouse model of skin regeneration. We used bioprinting technology to treat full-thickness skin wounds in nu/nu mice. AFS cells and bone marrow-derived mesenchymal stem cells (MSCs) were resuspended in fibrin-collagen gel and "printed" over the wound site. At days 0, 7, and 14, AFS cell- and MSC-driven wound closure and re-epithelialization were significantly greater than closure and re-epithelialization in wounds treated by fibrin-collagen gel only. Histological examination showed increased microvessel density and capillary diameters in the AFS cell-treated wounds compared with the MSC-treated wounds, whereas the skin treated only with gel showed the lowest amount of microvessels. However, tracking of fluorescently labeled AFS cells and MSCs revealed that the cells remained transiently and did not permanently integrate in the tissue. These observations suggest that the increased wound closure rates and angiogenesis may be due to delivery of secreted trophic factors, rather than direct cell-cell interactions. Accordingly, we performed proteomic analysis, which showed that AFS cells secreted a number of growth factors at concentrations higher than those of MSCs. In parallel, we showed that AFS cell-conditioned media induced endothelial cell migration in vitro. Taken together, our results indicate that bioprinting AFS cells could be an effective treatment for large-scale wounds and burns. STEM CELLS TRANSLATIONAL MEDICINE *2012;1:792–802*

INTRODUCTION

Extensive burns and full-thickness skin wounds can be devastating to patients, even when treated. There are an estimated 500,000 burns treated in the U.S. each year [1, 2]. The overall mortality rate for burn injury was 4.9% between 1998 and 2007, and medical costs for burn treatments approach $2 billion per year [3]. Globally, this statistic increases to 11 million injuries per year [4]. In addition to burns, full-thickness chronic wounds constitute a large patient base, and despite technological advancement of treatments, healing rates remain below 50% successful [5]. These nonhealing chronic wounds are estimated to affect 7 million people per year in the U.S., with yearly costs approaching $25 billion [6]. Patients who suffer from either of these types of injuries benefit from rapid treatments that result in complete closure and protection of the wounds. In particular, burn patients who receive delayed treatments often subject to extensive scarring that can result in negative long-term physiological effects.

Recent advances have been made in treatments for wound healing; however, the gold standard still used in the clinic is an autologous split-thickness skin graft. This involves removing a piece of skin from a secondary surgical site for the patient, stretching the skin, and reapplying the graft on the wound or burn. Although this treatment yields a reasonable clinical outcome, if the wound is extensive, then the number and size of donor sites are limited. Allografts are an additional option, but they suffer from the need of immunosuppressive drugs to prevent immune rejection of the graft. These limitations have thus led to the development of noncellular dermal substitutes, which are most often made up of a polymeric scaffold. Examples include Integra (Integra Life Sciences, Plainsboro, NJ, http://www.integralife.com) and Biobrane (UDL Laboratories, Rockford, IL, http://www.udllabs.com), and although such materials result in improved wound healing over untreated controls [7, 8], they are costly to produce and result in relatively poor cosmetic outcomes.

Recent advances in tissue engineering have led to more complex biological skin equivalents

that may yield more suitable wound treatment options for patients. Examples include cellularized graft-like products, such as Dermagraft (Advanced Biohealing, Westport, CT, http://www.dermagraft.com), Apligraf (Organogenesis, Canton, MA, http://www.organogenesis.com), and TransCyte (Advanced Biohealing, Westport, CT, http://www.transcyte.com). These products are generally composed of a polymer scaffold patch that is seeded with human fibroblasts and cultured in vitro prior to application. Unfortunately, these grafts are also expensive to produce and, as allografts, can suffer from the same immunological drawbacks discussed above. Alternatively, cell spraying and bioprinting technologies have recently been developed for wound treatment. In these approaches, cells are mixed in a hydrogel carrier vehicle and deposited over the wound via a spray nozzle or print-head.

Bioprinting has emerged as a flexible tool with potential in a variety of tissue engineering and regenerative medicine applications. Bioprinting can be described as robotic deposition that has the potential to build organs or tissues [9]. In general, bioprinting uses a computer-controlled printing device to accurately deposit cells and biomaterials into precise three-dimensional geometries in order to create anatomically correct structures. These devices have the ability to print cells (the "bio-ink") in the form of cell aggregates, cells encapsulated in hydrogels, or cell-seeded microcarriers. The polymers that provide structure or space-holding capabilities are serving as the supporting "bio-paper" [10, 11].

The cell source used in cellular therapies for wound healing is an important consideration that has implications in the cost, speed, and outcome of the treatments. Human keratinocytes are perhaps the optimal cell type to use. However, autologous and allogeneic keratinocytes suffer from the same drawbacks as their autologous and allogeneic skin graft counterparts, that is, secondary surgical sites and potential for rejection, respectively. This invites the question, can we use cells that are beneficial to wound healing but may be immunoprivileged even though they originate from an allogeneic source?

Mesenchymal stem cells (MSCs) have shown therapeutic potential for repair and regeneration of tissues damaged by injury or disease. In particular, MSC treatment of acute and chronic wounds results in accelerated wound closure, increased epithelialization, formation of granulation tissue, and angiogenesis [12]. MSCs have recently been shown to be also effective for improving in vivo skin expansion, a technique often used to create room for surgical implants that creates tissue damage and necessitates tissue regeneration [13]. Amniotic fluid-derived stem (AFS) cells are an attractive cell source for applications in regenerative medicine because of their high proliferation capacity, multipotency, immunomodulatory activity, and lack of significant immunogenicity [14, 15]. Unlike embryonic stem cells, AFS cells do not form teratomas when injected into immune-deficient mice. Furthermore, AFS cells remain stable and show no signs of transformation in culture. The isolation of AFS cells is a simpler process than that for isolation of MSCs, and large numbers of AFS cells can be isolated and expanded from as little as 2 ml of amniotic fluid. These cells proliferate rapidly with doubling times of 30–36 hours and do not require supportive feeder layers [14].

The immunomodulatory and high proliferation properties of AFS cells suggest that they can be used as an "off-the-shelf" cell therapy product for wound healing. Herein, we used a murine large skin wound model and bioprinting technology to deliver AFS cells in a fibrin-collagen hydrogel to the wound site. We hypothesized that AFS cells would facilitate wound healing and could thus be further considered for clinical applications of excessive skin wounds.

Materials and Methods

Hydrogel Preparation

To generate solutions that when printed formed robust gels, the components of fibrin were combined with collagen. Fibrinogen (Sigma-Aldrich, St. Louis, MO, http://www.sigmaaldrich.com) was dissolved in phosphate-buffered saline (PBS) to make a 50 mg/ml solution. Thrombin (Sigma-Aldrich) was dissolved in PBS to make a 20 IU/ml solution. Type I rat tail collagen (BD Biosciences, Bedford, MA, http://www.bdbiosciences.com) was diluted in ice-cold PBS to give a 2.2 mg/ml solution, after which the pH was adjusted to 7.0 using 1 N NaOH. All solutions were then sterile filtered with a 0.4-μm syringe filter. To form gels, the fibrinogen and collagen solutions were mixed together in a 1:1 ratio by volume. That mixed solution was then in turn mixed with the thrombin solution, after which the gel began to cross-link within 30 seconds.

Cell Culture and Cell Labeling

Multipotent stem cells were isolated from human amniotic fluid as previously described [14]. To achieve a relatively homogenous subpopulation, the cells were expanded in culture from a single clone. AFS cells can proliferate rapidly in culture without feeder cells for many passages, while maintaining chromosomal stability.

AFS cells (H1 clone, passage 16) and bone marrow-derived MSCs (passage 5; Lonza, Hopkinton, MA, http://www.lonza.com) were expanded in tissue culture plastic using 150 mm diameter dishes (37°C, 5% CO_2) until 75% confluence with Chang's media (α-minimal essential medium [α-MEM] with 18% Chang B [Irvine Scientific, Santa Ana, CA, http://www.irvinesci.com], 15% embryonic stem cells screened-fetal bovine serum [ES-FBS] [HyClone, Logan, UT, http://www.hyclone.com], 2% Chang C [Irvine Scientific]) and α-MEM with 10% ES-FBS, respectively. Cells were detached from the substrate with Accutase (Innovative Cell Technologies, San Diego, CA, http://www.innovativecelltech.com) and counted prior to centrifugation. Cells were resuspended in the fibrinogen/collagen solution at a density of 16.6 million cells per milliliter.

For visualization and tracking of the printed cells, AFS cells and MSCs were genetically labeled with green fluorescent protein (GFP), using a lentivirus vector carrying the GFP gene (Lenti-GFP), with a standard procedure. Labeling efficiency (70%–80%) was verified by fluorescence-activated cell sorting. The cells were then expanded as needed to reach sufficient numbers for bioprinting.

Bioprinting

In preparation for printing, AFS cells and MSCs were separately suspended in the fibrinogen/collagen solution at a density of 16.6 million cells per milliliter and placed on ice. While under anesthesia, a single full-thickness skin wound (2.0 $\times$ 2.0 cm) was surgically created with scissors on the mid-dorsal region of nu/nu mice. A bioprinting device developed in-house [16] was used for cell deposition using fibrin/collagen gels. The device consists of a carriage with three-axis movement capability in which is housed

the main print head. The print head is made up of a set of pressure-driven nozzles through which the hydrogel solutions, with or without cells, are printed, and an additional set of high-pressure nozzles through which secondary solutions, such as cross-linking solutions, can be printed. The printable hydrogel solutions are housed in swappable cartridges in line with the back-pressure and the print nozzles. The printing process is then controlled using software also developed in-house.

For treatment, the bioprinter was used to deposit two layers of a fibrin-collagen gel by depositing a layer of thrombin, a layer of fibrinogen/collagen, a second layer of thrombin, a second layer of fibrinogen/collagen, and a final layer of thrombin. Equal amounts of the two solutions were used (0.3 ml), resulting in 5×10^6 AFS cells or MSCs deposited per wound. Additionally, gel-only treatments, containing no cells, were administered. Triple antibiotic (bacitracin zinc, neomycin sulfate, polymyxin-B sulfate; Medique Products, Fort Myers, FL, http://www.mediqueproducts.com) was applied over each wound after gelation, followed by a Tegaderm bandage (3M, St. Paul, MN, http://www.3m.com). Finally, a custom-made bandage was sutured in place in order prevent the Tegaderm from being removed. Wound size was documented by taking photographs immediately after surgery and again at 7 and 14 days ($n = 5$). Animals were euthanized at 7 and 14 days, and the regenerated skin was harvested for histological analysis. Additionally, several mice were euthanized at 1 and 4 days for cell tracking purposes and to evaluate the consistency and distribution of bioprinted cells by confocal microscopy.

Gross Histology: Wound Closure, Contraction, and Re-Epithelialization

Wound closure, contraction, and re-epithelialization percentages were calculated using photographs and histological examination of the wounds, taken at the time of surgery, day 7, and day 14. Using ImageJ software, the original wound area was defined as A, the clearly re-epithelialized (but thinner) skin area was defined as B, and the remaining unclosed wound was defined as C. Percentage of wound closure was defined as $C/A \times 100\%$, percentage of contraction of the wound was defined as $(A - B)/A \times 100\%$, and percentage of re-epithelialization was defined as $(B - C)/B \times 100\%$.

Histology

Harvested skin tissues were first rolled around a syringe needle prior to being fixed overnight in 4% paraformaldehyde. Samples were then washed in PBS three times for 30 minutes per wash, after which the samples were transferred to 30% sucrose for an overnight incubation at 4°C. The rolled tissues were then sliced in half and flash frozen in Tissue-Tek OCT Compound (Sakura Finetek, Torrance, CA, http://www.sakura.com) blocks in liquid nitrogen. A cryotome (Leica, Heerbrugg, Switzerland, http://www.leica.com) was used to generate 6-μm sections made up of the entire cross-sections of the regenerating wounds. These slides were stored at −20°C until histological procedures were performed.

Sections were stained with hematoxylin and eosin for histology, and slides were imaged under light microscopy. Attention was paid to the presence of blood vessels in the regenerated tissue and re-epithelialization of keratinocytes across the surface of the wound area.

Immunohistochemistry

Immunohistochemical (IHC) staining with smooth muscle actin (SMA) was used to visualize smooth muscle cells (SMCs) in mature blood vessels in the regenerating skin, or with von Willebrand factor (vWF) to visualize endothelial cells in newly formed capillaries and lining the mature blood vessels. For IHC, all incubations were carried out at room temperature unless otherwise stated. Slides were warmed at 60°C for 1 hour to increase bonding to the slides. Antigen retrieval was performed on all slides and achieved with incubation in proteinase K (Dako, Carpinteria, CA, http://www.dako.com) for 5 minutes.

For SMA staining, sections were permeabilized with 0.05% Triton X-100 in PBS (PBST) for 5 minutes. Endogenous peroxidase activity was blocked with 3% hydrogen peroxide solution in methanol for 30 minutes. Nonspecific antibody binding was minimized by incubating sections for 10 minutes in Protein Block Solution (Abcam, Cambridge, U.K., http://www.abcam.com). Sections were incubated for 90 minutes in a humidified chamber with primary anti-α-SMA antibodies (catalog no. ab5694; Abcam) at a 1:200 dilution. Following primary incubation, slides were washed three times in PBS for 5 minutes. Sections were then incubated for 30 minutes with biotinylated secondary antibody solution at a 1:400 dilution. After washing, sections were incubated with horseradish peroxidase-streptavidin RTU (Vector Laboratories, Burlingame, CA, http://www.vectorlabs.com) for 30 minutes. Visualization of immunoreactivity was achieved by incubating sections in the 3,3′-diaminobenzidine peroxidase substrate kit (Vector Laboratories) for 1–2 minutes. The sections were washed in PBS, counterstained with hematoxylin, dehydrated, and coverslipped. Native skin samples were present as positive controls and were used for comparison. Negative controls were set up at the same time as the primary antibody incubations and included incubation with PBS in place of the primary antibody. No immunoreactivity was observed in these negative control sections.

For vWF staining, immunofluorescent staining was used. Nonspecific antibody binding was blocked in 10% normal donkey serum (NDS) with 50 μg/ml anti-mouse IgG Fab fragments (Jackson Immunoresearch Laboratories, West Grove, PA, http://www.jacksonimmuno.com) for 60 minutes. Sections were incubated for 90 minutes in a humidified chamber with the primary anti-vWF antibodies (catalog no. AB7356; Millipore, Billerica, MA, http://www.millipore.com) at a 1:200 dilution in 3% NDS. Following primary incubation, slides were washed three times in PBS for 5 minutes. Sections were then incubated for 60 minutes with DyLight 594-conjugated AffiniPure donkey anti-rabbit IgG secondary antibodies in a 1:200 dilution in 3% NDS. The sections were washed in PBS, counterstained with 4′,6-diamidino-2-phenylindole (DAPI), and coverslipped with Prolong Gold Antifade (Invitrogen, Carlsbad, CA, http://www.invitrogen.com). Positive and negative controls were performed in the same manner as described above.

Quantification of neovascularization was done by determining the microvessel density (MVD) and average vessel diameter (AVD) in hematoxylin and eosin (H&E)-stained wound cross-sections. To do this, ImageJ software was used to perform measurements on histological images. For MVD, first the cross-sectional area of tissue in the image was determined. Within that area the number of vessels was counted. MVD values were calculated by dividing the area by the number of vessels, after which the average MVD per group was determined. For AVD, vessels were selected at random from

histological images taken of each animal. To calculate each individual vessel diameter, the perimeter of the vessel was traced and ImageJ was used to calculate the cross-sectional vessel area. The diameter, D, was then derived by the equations Area $= \pi r^2$ and D $=$ 2r, after which the AVD was determined.

Fluorescence Imaging of Cells

To investigate whether the deposited cells remain in the regenerating skin long-term after the bioprinting, GFP-transfected AFS cells and MSCs cells were used. Animals were euthanized on days 1, 4, 7, and 14 after cell bioprinting, and skin samples were harvested and prepared for histology as described above. Samples were then washed three times in PBST, counterstained with DAPI, and washed three times before mounting with Prolong Gold Antifade reagent (Invitrogen). Sections were imaged using a fluorescence microscope, and representative images were recorded.

Cell-Conditioned Media

AFS cells and MSCs were cultured as described above in 150 mm diameter dishes until 75% confluence. At this point, the medium was aspirated and the cells were washed with PBS to remove any remaining serum. Next, 10 ml of serum-free α-MEM was added to each dish. The cells were returned to the incubator for 3 additional days, after which the conditioned medium was collected. The conditioned medium samples were concentrated by lyophilization, and analyzed for growth factor and cytokine content using a Quantibody Human Growth Factor Array (RayBiotech, Norcross, GA, http://www.raybiotech.com).

In Vitro AFS Cell-Induced Transwell Migration Assays of Human Umbilical Vein Endothelial Cells

To investigate the effect of AFS cells to induce migration of endothelial cells for angiogenesis, Transwell (Corning Enterprises, Corning, NY, http://www.corning.com) migration assays were performed using human umbilical vein endothelial cells (HUVECs) as the migrating populations. H1 AFS cells were expanded as described above, before being plated into collagen-coated soft substrates (2 kPa stiffness, Excellness Biotech, Lausanne, Switzerland, http://www.excelleness.com) or plastic 24-well plates at a density of 100,000 cells per well. The aforementioned soft substrates were implemented to provide in vitro substrates that might better mimic the mechanical properties experienced by the AFS cells in the in vivo portion of this study. HUVECs were expanded on tissue culture plastic using 150 mm diameter dishes coated with fibronectin (37°C, 5% CO_2) until 75% confluence with endothelial basal medium containing 2% FBS (Lonza). After 24 hours of H1 AFS culture in the wells, HUVECs were detached from the substrate with Accutase, counted prior to centrifugation, and seeded into Transwell inserts that had been coated in fibronectin at a density of 50,000 cells per insert. The inserts were then placed in the previously prepared H1-seeded soft 2-kPa and plastic wells, as well as cell-free control wells with Chang's media.

After 4 hours, inserts were fixed with 4% paraformaldehyde for 15 minutes. Cells still attached to the interior side of the inserts (nonmigratory) were removed with cotton swab applicators. Cells attached to the outside of the insert membranes were stained by placing each insert in 0.05% crystal violet solution for 20 minutes. Inserts were then washed two times in distilled water to remove excess dye. The insert membranes were then cut out of the inserts and mounted on glass slides for photography and analysis of migrated cells.

Results

Bioprinting of Cells onto Skin Wounds

The bioprinting procedure, depicted in Figure 1A, consistently yielded a fibrin/collagen gel that provided 100% coverage over the wound area and formed a tight seal with the skin at the edges of the excisional wound (not shown). To assess the distribution of cells, delivered to the wound by the bioprinting procedure, confocal microscopy of gel/tissue at day 1 was used to visualize the fluorescently labeled AFS cells. Figure 1B shows a uniform distribution of cells in a representative image spanning an approximately 900 $\times$ 900 μm area of the harvested tissue. Figure 1C shows a cross-sectional view (z axis) of the same sample, in which the vertical distribution of cells is consistent across the sample.

Wound Closure

Wound closure was determined using photographs taken at week 0 (the time of surgery), week 1, and week 2 (Fig. 2A). ImageJ software was used to quantify wound closure (Fig. 2B). Because of variations in the starting area of individual wounds, all measurements were converted to percentages of the corresponding wound sizes from the wound size at time of surgery. At week 1, AFS-treated mice showed an average of 42% unclosed wounds and MSC-treated mice showed an average of 44% unclosed wounds. These values were not significantly different from each other but were significantly lower than those of mice treated with gel only, which had an average of 77% unclosed wounds ($p < .01$). At week 2, AFS-treated mice showed an average of 3% unclosed wounds and the MSC-treated mice showed an average of 2% unclosed wounds. These values were significantly lower than those of mice treated with gel only, which had an average of 13% unclosed wounds ($p < .05$). At all time points, wound closure in the AFS cell- and MSC-treated groups was not significantly different.

Contraction and Keratinocyte Re-Epithelialization

Wound contraction and re-epithelialization was determined by comparing the gross histology of the wounds at the time of surgery with that of 1 and 2 weeks after the surgery (Fig. 3A, 3B). At week 1, AFS cell- and MSC-treated wounds had contracted 44% and 43%, respectively, which was significantly higher than the 17% contraction observed in gel-only-treated wounds ($p < .01$). At week 2, only the MSC-treated wounds were significantly more contracted than gel-only-treated wounds ($p < .05$), at 83% compared with 73%. AFS cell- and MSC-treated groups had greater re-epithelialization at both time points. At week 1, AFS cell- and MSC-treated wounds had 25% and 21% re-epithelialization, respectively, compared with 7% re-epithelialization in gel-only-treated wounds ($p < .01$). At week 2, AFS cell- and MSC-treated wounds had 84% and 89% re-epithelialization, respectively, compared with 51% re-epithelialization in gel-only-treated wounds ($p < .01$ and $p < .05$, respectively).

Additionally, H&E-stained histological sections of skin samples, harvested at week 2, showed clear differences in the quality of the epidermal layers near the center of the wound areas in each group. In gel-only-treated wounds, poorly defined epidermal layering was observed (Fig. 3C). In fact, the structural integrity of the regenerated skin was poor, resulting in crumbling during cryosectioning. In contrast, MSC-treated wounds (Fig. 3D)

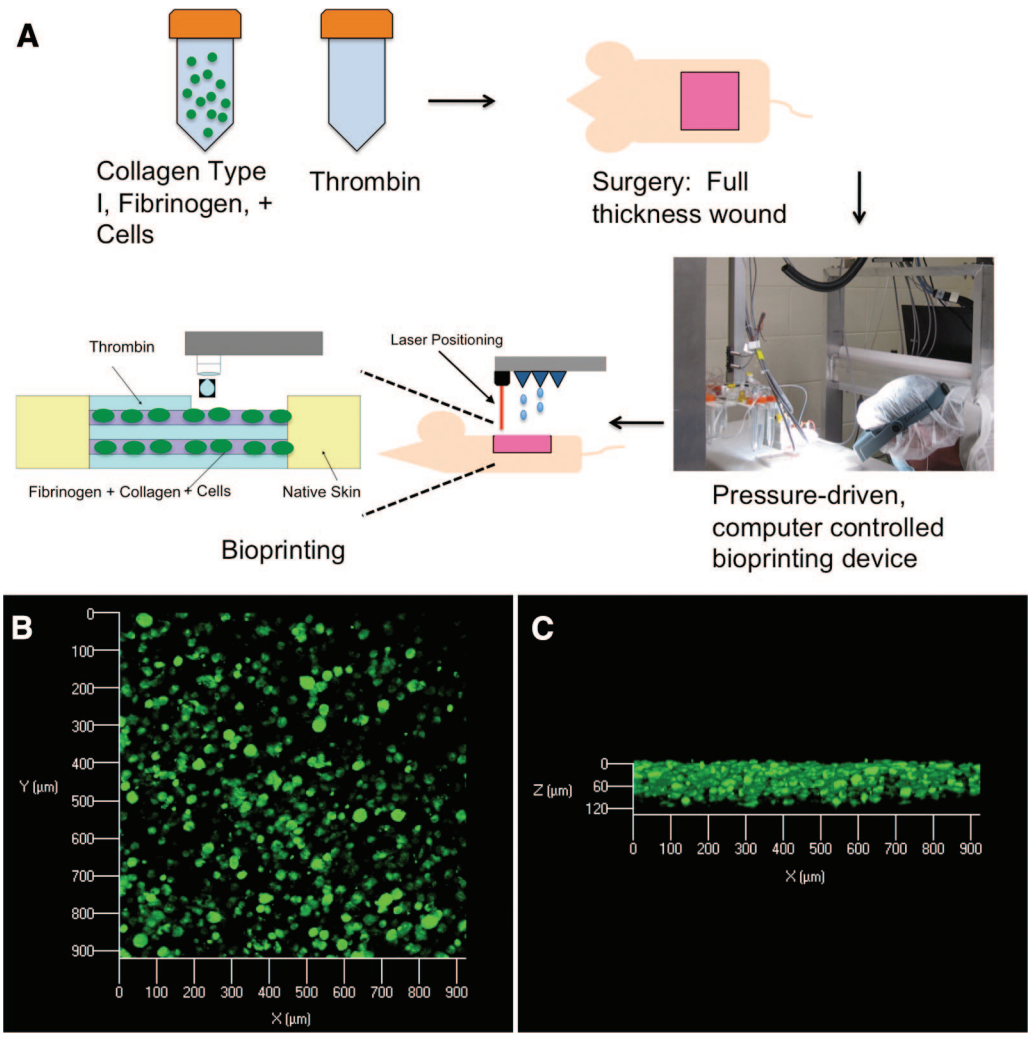

Figure 1. Bioprinting stem cells for treatment of skin wounds. **(A):** A schematic describing the approach by which amniotic fluid-derived stem (AFS) cells are bioprinted in order to increase healing of a full-thickness skin wound. Wounds containing the deposited gels with green fluorescent protein-tagged AFS cells were harvested 24 hours postprinting and analyzed with confocal microscopy. Images revealed evenly distributed cells in the gels, as viewed from above **(B)** or from the side **(C)**.

and AFS cell-treated wounds (Fig. 3E) showed well-defined, organized epidermal layers of the regenerated skin.

Histological examination of the wound site at multiple times after deposition of human AFS cells and MSCs showed no indications of immune cell activity. Although the nu/nu (NU/J) mice used in this study lack mature T cells and therefore suffer from a lack of cell-mediated immunity and show only a partial defect in B-cell development (probably due to the absence of functional T-cells), their innate immunity is intact, with normal circulating levels of natural killer cells, dendritic cells, monocytes, and macrophages, as well as normal complement activity. This result may be due to the immunomodulatory activity of both AFS cells and MSCs but could be a result of the immune-compromised mouse model used. As such, further examination of these cells in an immune-competent animal is necessary.

Neovascularization of Regenerating Skin

H&E-stained histological sections of regenerating skin tissues illustrate the presence of blood vessels (Fig. 4A–4F). At week 1, gel-only-treated wounds remained relatively thin, with blood vessels primarily only visible in the subcutaneous adipose tissue (Fig. 4A). In contrast, MSC-treated (Fig. 4B) and AFS cell-treated (Fig. 4C) wounds showed noticeably thicker regenerating tissue. Furthermore, a greater number of blood vessels was observed in the regenerating skin in these groups, especially in the AFS cell-treated one. At week 2, the difference in the number of visible blood vessels between groups remained. Gel-only-treated wounds showed the fewest vessels (Fig. 4D), followed by MSC-treated wounds (Fig. 4E), whereas AFS cell-treated wounds showed the largest number of blood vessels (Fig. 4F). Additionally, vessels in the AFS cell-treated tissues appeared noticeably larger.

To quantify these observations, MVD and AVD values were determined from the histological sections by ImageJ software (Fig. 4G, 4H). Anti-vWF immunostaining confirmed the vascular structures (not shown). At week 1, MVD values in MSC and AFS groups were both significantly greater than that of the gel-only group ($p < .05$), whereas AVD values were not significantly different. At week 2, MVD values of the AFS group were significantly greater than those of both MSC and gel-only groups ($p < .05$). In addition, AVD values of the AFS group significantly increased and were significantly greater than those of the MSC group ($p < .05$), whose AVD values were significantly greater than those of the

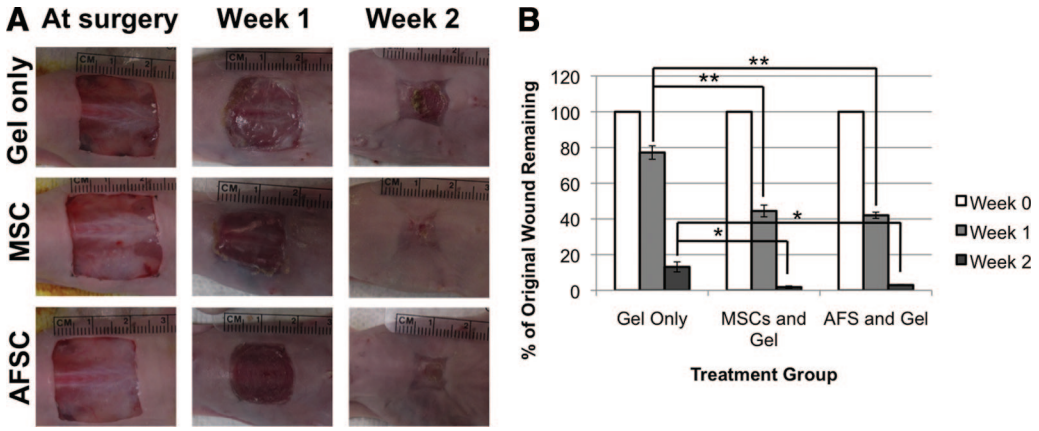

Figure 2. Wound closure rates are increased in AFS cell- and MSC-treated mice. **(A):** Gross histology images illustrating wound closure in gel-only, MSC, and AFS treatments. **(B):** Percentage of unclosed wound remaining at surgery, 1 week, and 2 weeks. Significance: *, $p < .05$; **, $p < .01$. Abbreviations: AFS, amniotic fluid-derived stem; AFSC, amniotic fluid-derived stem cell; MSC, mesenchymal stem cell.

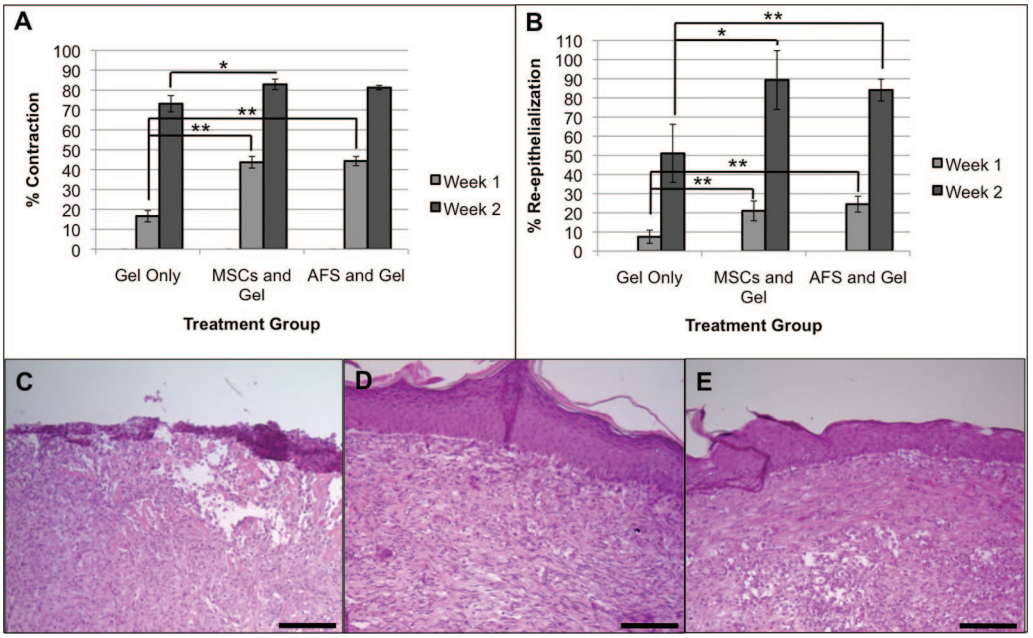

Figure 3. Contraction and re-epithelialization rates are increased in AFS cell- and MSC-treated mice. Quantification of contraction **(A)** and re-epithelialization **(B)** at surgery, 1 week, and 2 weeks. Significance: *, $p < .05$; **, $p < .01$. Re-epithelialization was visualized by the extent of formation of keratinocyte layers in hematoxylin and eosin-stained tissue sections. **(C):** Poorly defined epithelium in the group treated with gel only. **(D, E):** Well-defined and structurally robust epithelium in MSC-treated **(D)** and AFS-treated **(E)** groups. Scale bars = 50 μm. Abbreviations: AFS, amniotic fluid-derived stem; MSC, mesenchymal stem cell.

gel-only group ($p < .05$). This change in AVD suggested stabilization and maturation of the new vessels over time.

To further investigate vessel maturation, histological sections were stained for SMA (Fig. 4I–4K) and extravasation of red blood cells (RBCs) was examined in these sections (Fig. 4L–4N). In the gel-only group (Fig. 4I) very few SMA-stained SMCs were observed. Although many SMA-stained SMCs were observed in the MSC group (Fig. 4J), they did not form a complete circle around the vascular structures. In contrast, in the AFS group (Fig. 4K), complete circles of strongly stained SMCs were observed around the vascular structures, further suggesting blood vessel maturation in this group. Furthermore, large numbers of RBCs were observed in the regenerating skin tissue in the gel-only (Fig. 4L) and MSC (Fig. 4M) groups, suggesting extravasation from immature, "leaky" vasculature. In contrast most RBCs were contained inside the vasculature in the regenerating skin in the AFS cell group (Fig. 4N).

Fluorescence Imaging of AFS Cells and MSCs

Fluorescence imaging of GFP-expressing AFS cells and MSCs was carried out in order to track the cells in the regenerating skin tissue, following cell bioprinting. Skin samples were harvested on days 1, 4, 7, and 14 after surgery and examined by fluorescent microscopy (Fig. 5). The tissues were stained with DAPI to reveal all cells in the tissue. At day 1 the large number of GFP-labeled cells were visible in the wounds of the AFS cell and MSC groups. In both cell types, this number decreased by roughly 50% at day 4, and only a few GFP-labeled cells were seen at day 7. In tissues harvested at day 14 no GFP-labeled cells could be detected. Furthermore, GFP-labeled cells

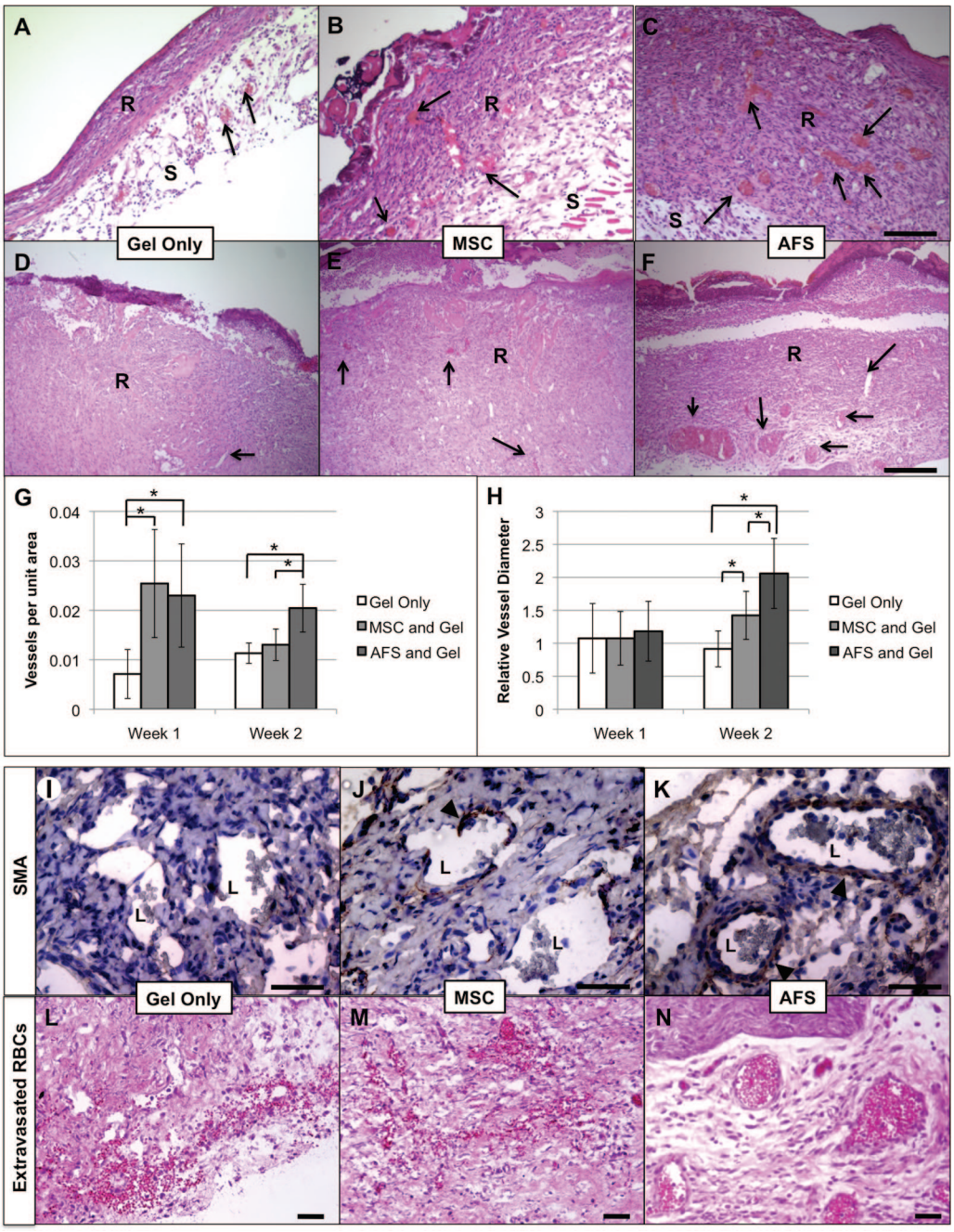

Figure 4. AFS cells induce neovascularization and blood vessel maturation in vivo. Hematoxylin and eosin staining revealed thicker regenerating tissue with more blood vessels in the AFS and MSC groups compared with the gel-only group. **(A–C):** Week 1; **(D–F):** week 2. **(A, D):** Gel-only; **(B, E):** MSC; **(C, F):** AFS. Arrows: vessels. AFS cells increased the number of newly formed vessels and induced formation of larger vessels. Microvessel density **(G)** and vessel diameter **(H)** were quantified using histology images and ImageJ software. Significance: $*$, $p < .05$. AFS cells induced formation of mature blood vessels. SMA staining was seen around blood vessels in regenerated tissues of the gel-only **(I)**, MSC **(J)**, and AFS **(K)** groups. Arrows: cells expressing SMA. Extravasated RBCs were present in the gel-only **(L)** and MSC groups **(M)** but not in the AFS group **(N)**. Scale bars = 50 μm. Abbreviations: AFS, amniotic fluid-derived stem; L, lumen; MSC, mesenchymal stem cell; R, regenerated tissue; RBC, red blood cell; S, subcutaneous tissue; SMA, smooth muscle actin.

remained at the wound surface and did not migrate into the underlying tissue. These data indicate that the printed cells remained transiently in the tissue, and did not permanently integrate. These observations suggest that wound closure and neovascularization, observed in groups treated with bioprinting of cells, may be due to secretion of trophic factors from the cells rather than cell integration in the regenerating skin.

Analysis of Growth Factors in Conditioned Media of AFS Cells and MSCs

Proteomics analysis of AFS-conditioned media (CM) and MSC-CM illustrated differences in their growth factor secretory profiles (Table 1). In general, AFS-CM contained more growth factors at higher concentrations. Although MSC-CM had twofold

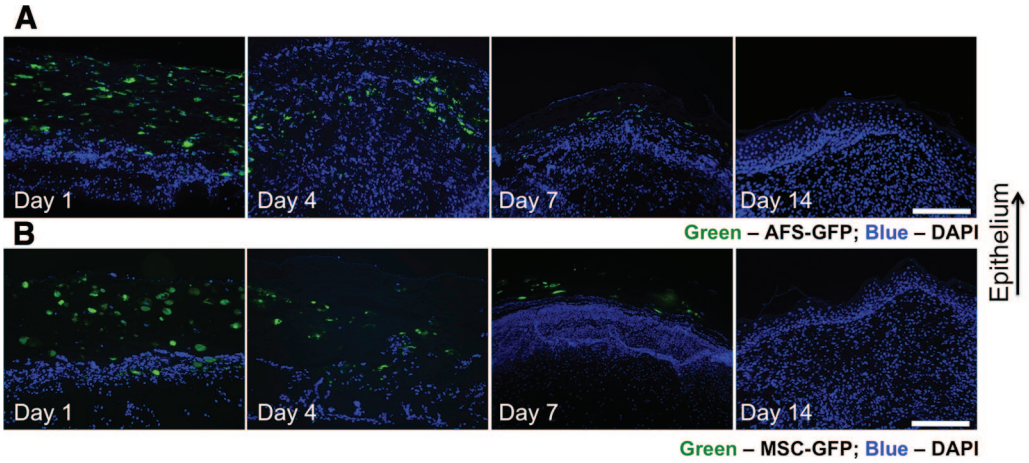

Figure 5. AFS cells and MSCs are transient in the regenerating wound and do not permanently integrate into the tissue. Regenerating skin was harvested at days 1, 4, 7, and 14 in order to determine the presence of labeled cells. GFP-labeled AFS cells **(A)** and MSCs **(B)** were visible in decreasing numbers over the time course of the experiment. Green: GFP-expressing AFS or MSCs; blue: nuclear staining, DAPI. Scale bars = 50 μm. Abbreviations: AFS, amniotic fluid-derived stem; GFP, green fluorescent protein; MSC, mesenchymal stem cell; DAPI, 4′, 6-diamidino-2-phenylindole.

Table 1. Quantification of growth factors secreted by AFS cells and MSCs in vitro: growth factor analysis of conditioned media

Growth factor	AFS cells (pg/ml)	MSCs (pg/ml)
bFGF	459	—[a]
FGF-7	1,507	3,106
GDF-15	95	50
GDNF	21	—[a]
HGF	218	—[a]
IGFBP-2	1,490	4,167
IGFBP-3	8,852	—[a]
IGFBP-4	65,249	987
IGFBP-6	17,470	—[a]
NT-3	530	—[a]
OPG	1,882	7,852
PDGF-AA	—[a]	176
PlGF	—[a]	18
VEGF	5,006	10,953

AFS cells secrete more growth factors than MSCs. The presence of growth factor concentrations in AFS- and MSC-conditioned media was determined by proteomic arrays.
[a]Growth factors were undetectable.
Abbreviations: AFS, amniotic fluid-derived stem; bFGF, basic fibroblast growth factor; FGF, fibroblast growth factor; GDF, growth differentiation factor; GDNF, glial cell-derived neurotrophic factor; HGF, hepatocyte growth factor; IGFBP, insulin-like growth factor-binding protein; MSC, mesenchymal stem cell; NT, neurotrophin; OPG, osteoprotegerin; PDGF, platelet-derived growth factor; PlGF, placental growth factor; VEGF, vascular endothelial growth factor.

more vascular endothelial growth factor (VEGF) than AFS-CM, it did not contain basic fibroblast growth factor (bFGF) or hepatocyte growth factor (HGF), found in AFS-CM. bFGF levels in AFS-CM were about 500 pg/ml CM, whereas VEGF levels in MSC-CM were about 5–10 ng/ml. In addition to bFGF and HGF, members of the insulin-like growth factor-binding protein superfamily were expressed at much higher levels in AFS-CM compared with MSC-CM.

Endothelial Cell Migration in Response to AFS Cell-Secreted Growth Factors

To test the activity of the angiogenic growth factors secreted by AFS cells, we performed an in vitro migration assay. To mimic the environment in which the AFS cells were bioprinted onto the wounds, the AFS cells were cultured on soft substrates (gels), and compared with AFS cells cultured in standard tissue culture plastic dishes. After 24 hours of culture, HUVECs, seeded inside Transwell inserts, were placed above the AFS cell cultures, as well as above nonseeded culture dishes. The numbers of HUVECs that migrated across the filter support of the insert was determined after 4 hours (Fig. 6A–6D). Significantly more HUVECs migrated in inserts placed over AFS cells that were cultured on soft 2-kPa substrates, compared with those on plastic, or in wells without cells ($p < .05$).

Discussion

Extensive skin wounds, including severe burns, can be devastating to patients, even when treated, and have a huge financial burden on the medical establishment. These patients require a treatment that results in complete closure and protection of the wound. Although many improvements have been made in treatments for such wounds, the autologous split-thickness skin graft is still the best available treatment. The bioprinted AFS cell therapy approach presented here may have the potential to address the clinical need for more effective treatment of burns and skin wounds. In this study we bioprinted banked cells with immunomodulatory characteristics using a fast deposition method to support quick and complete wound coverage in situ. We found that AFS cells deposited in a collagen/fibrin gel accelerated closure of full-thickness wounds in mice faster than gel-only controls and were as effective as MSC treatments. Additionally, the AFS treatment induced increased neovascularization and blood vessel maturation over the course of the study. Based on the analysis of cell-conditioned media and an in vitro endothelial cell migration assay, it is likely that these effects of the AFS cells are due to secretion of a number of trophic factors important for wound healing and angiogenesis.

An optimal treatment for burns or skin wounds would use an off-the-shelf approach for fast application. Quick response is especially important for victims with extensive burns. Additionally, the treatment should not create a secondary surgical site, it should not be rejected by the patient's immune system, and it needs to form a robust covering over the wound quickly.

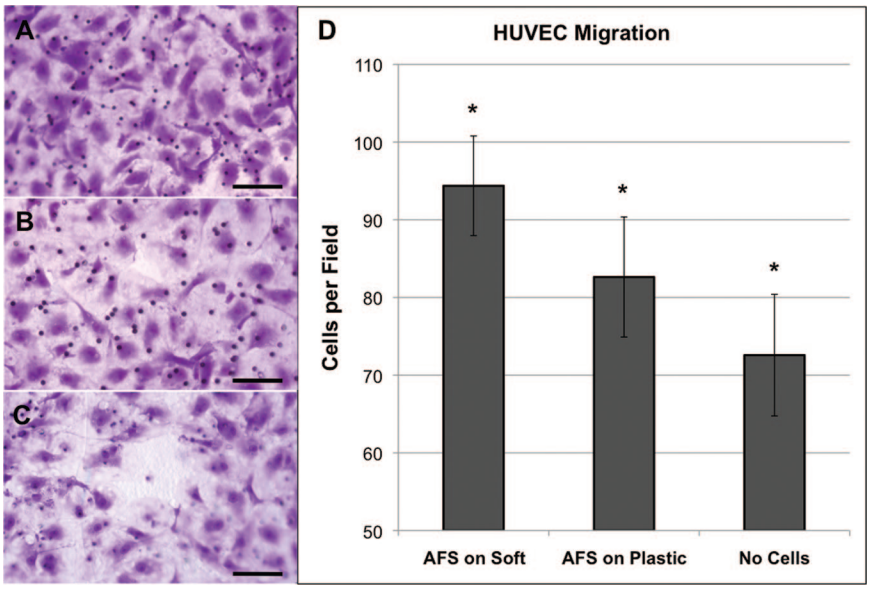

Figure 6. AFS cells induce endothelial cell migration in vitro. AFS cells cultured on soft surfaces increased migration rates of HUVECs. **(A–C):** Crystal violet-stained HUVECs that migrated through Transwell inserts toward AFS cells cultured on soft in vivo-like substrates **(A)**, plastic **(B)**, or Chang's media only **(C)**. **(D):** Average number of observed migrated HUVECs per field of view. Significance: ∗, p values between all pairwise comparisons between the three groups were less than .05. Scale bars = 50 μm. Abbreviations: AFS, amniotic fluid-derived stem; HUVEC, human umbilical vein endothelial cell.

Multipotent and expandable cells were first isolated from amniotic fluid by De Coppi et al. [14]. AFS cells express both embryonic stem cell and adult stem cell markers and can be expanded for more than 250 passages [14, 17, 18]. These cells can be induced to differentiate into cells that represent each germ layer, such as adipogenic, osteogenic, myogenic, endothelial, neuronal, hepatic, and chondrogenic lineages. Because of their location along the developmental timeline—they are "younger" than adult stem cells, in a developmental sense—AFS cells may have increased differentiation and expansion potential compared with MSCs [19]. We explored the use of AFS cells in this study for several reasons: AFS cells are highly expandable, allowing effective cell banking, further supporting the rationale for using them as an off-the-shelf treatment; AFS cells showed a degree of immunomodulatory activity [15] and thus might not be rejected in the wound environment; and AFS cells, like other MSCs, were shown to secrete growth factors and cytokines that have an anti-inflammatory activity and that aid in wound healing and tissue regeneration [20]. In the work presented here, we showed that AFS cells were equally effective as bone marrow-derived MSCs at increasing wound closure and re-epithelialization rates in full-thickness wounds. However, AFS cells induce stronger angiogenesis compared with MSC-treated groups and gel-only groups. Not only were microvessel density and average vessel diameter greater, but also smooth muscle actin stains verified that these blood vessels were mature and stable. In gel-only and MSC groups, the presence of more extravasated red blood cells suggested less mature vessel formation than in the AFS group. Immunofluorescence of GFP-tagging AFS cells and MSCs revealed that both types of printed cells decreased in number and were mostly gone by day 7. In this study we did not investigate the specific fate of the AFS cells and MSCs. There are several potential fates, including apoptosis, clearance by macrophages, and migration to other regions of the animal. We plan to investigate this phenomenon in future studies as part of preclinical studies, as cell fate is an important consideration.

In addition to their transiency, we did not observe migration of the delivered cells into the underlying tissue or colocalize with new vasculature. These results suggest that secretion of trophic factors was probably responsible for the wound closure rates and induced neovascularization, as opposed to direct cell integration into the new tissue. Indeed, AFS cells have been shown to be proangiogenic in other studies. Cytokines from AFS-conditioned media induced endogenous repair in ischemic full-thickness skin flaps in a rat model [21] and induced neovascularization in a hind limb ischemic mouse model [22]. Additionally, a functional in vitro assay demonstrated that AFS cells could successfully induce migration of endothelial cells across Transwell membranes. Whereas cell therapy provides a dynamic treatment with sustained growth factor release over time, conditioned medium offers only a one-time administration of growth factors that would likely result in a single burst response of bioactivity that would diminish after a short time. Thus, AFS cell therapy can probably result in a better wound healing treatment than the application of concentrated conditioned medium.

MSCs are being explored with increased frequency as potential wound healing treatments for clinical use application [23]. A large body of work has demonstrated that topical delivery of these cells generally improves wound healing rates and appears to act through interactions with vascular cells and immunomodulation [24]. For example, application of autologous bone marrow-derived cells increases neovascularization and healthy extracellular matrix formation while decreasing granulation tissue formation in a rabbit wound model [25]. Efficacy of MSC treatments can be further augmented by choosing an appropriate delivery vehicle. In one such example, similar to the study presented here, MSCs were delivered to wounds in a collagen-based gel. The gel environment increased MSC secretion of trophic factors and expression of transcription factors associated with stem cells, while accelerating the wound healing process [26].

As mentioned above, we did not observe migration and integration of the GFP-tagged AFS cells and MSCs into the regenerated skin. Although the results of using cells were significantly more efficacious than cell-free treatments, it might still be beneficial to increase cell migration to provide structural support for the regenerating skin tissue. It is possible that the mobility of the printed cells was limited by the carrier (collagen/fibrin gel) material. Collagen and fibrin are materials that are extremely cell-adherent and may have prevented cells from being mobile, potentially limiting the full potential of the printed cells.

Furthermore, collagen, in particular, naturally contracts as it cross-links into a gel. This could be detrimental to the natural healing process by causing too much contraction and thus potential fibrosis and scarring. Perhaps a hydrogel carrier vehicle that is more cell-permissive and less contractile is more appropriate, such as hyaluronic acid (HA) or polyethylene glycol diacrylate gels. Additionally, there exist natural polymers, such as HA, that are naturally anti-inflammatory and therefore may further improve our bioprinting treatment. To this end we are performing hydrogel screening studies to identify materials that would support cellular infiltration inside the regenerating tissue. Another avenue we are interested in exploring is combinatorial cell therapies. In particular, we might combine AFS cells with skin cells such as keratinocytes. In this approach we hope to more quickly establish a robust epithelial layer in the regenerating tissue while retaining all of the beneficial effects of AFS cell deposition.

Conclusion

Bioprinting is a novel technology to deliver cells within a polymer gel to a full-thickness skin wound. Bioprinting provides the ability to deliver cells in a fast, off-the-shelf manner, facilitating quick wound coverage and closure, which is critical in cases of large full-thickness wounds or burns. To date, a complete organ has not been printed, but it remains the primary long-term goal of bioprinting. A number of bioprinting approaches have been recently explored, primarily with the ultimate goal being the production of vascular structures. Cell aggregates and cell rods have been printed layer-by-layer into tubular formations supported by cell-free rods, after which the cell aggregates and rods fuse into singular structures, showing the feasibility of one method for printing cellularized tubular structures [27, 28]. Other approaches rely on hydrogels with specific mechanical properties and cross-linking chemistries to facilitate extrusion to also build cellularized tubular structures [29, 30]. The research presented here demonstrates that stem cell bioprinting in a hydrogel carrier is a promising approach for an effective wound healing therapy in clinical applications. Ultimately, bioprinter-mediated deposition of cells in hydrogels has the potential to build tissues and organs from the ground up.

Acknowledgments

This research was supported by NIH National Institute of Biomedical Imaging and Bioengineering Grant 1R01-EB008009 and the Armed Forces Institute for Regenerative Medicine ET-1 Grant. We acknowledge Dr. Kyle Binder for his role in designing and building the bioprinting device used in these studies, as well as Dr. Mark Pettenati for karyotypic analysis of the amniotic fluid-derived stem cells.

Author Contributions

A.S. and D.M.: conception and design, collection and/or assembly of data, data analysis and interpretation, manuscript writing; E.K.: collection and/or assembly of data, data analysis and interpretation; A.A.: conception and design, final approval of manuscript; J.D.J.: conception and design, data analysis and interpretation; J.Y.: conception and design, data analysis and interpretation, final approval of manuscript; S.S.: conception and design, data analysis and interpretation, manuscript writing, final approval of manuscript.

Disclosure of Potential Conflicts of Interest

The authors indicate no potential conflicts of interest.

References

1 Cherry DK, Hing E, Woodwell DA et al. National Ambulatory Medical Care Survey: 2006 summary. Natl Health Stat Report 2008:1–39.

2 Pitts SR, Niska RW, Xu J et al. National Hospital Ambulatory Medical Care Survey: 2006 emergency department summary. Natl Health Stat Report 2008:1–38.

3 Miller SF, Bessey P, Lentz CW et al. National burn repository 2007 report: A synopsis of the 2007 call for data. J Burn Care Res 2008; 29:862–870; discussion 871.

4 Peck MD. Epidemiology of burns throughout the world. Part I: Distribution and risk factors. Burns 2011;37:1087–1100.

5 Kurd SK, Hoffstad OJ, Bilker WB et al. Evaluation of the use of prognostic information for the care of individuals with venous leg ulcers or diabetic neuropathic foot ulcers. Wound Repair Regen 2009;17:318–325.

6 Sen CK, Gordillo GM, Roy S et al. Human skin wounds: A major and snowballing threat to public health and the economy. Wound Repair Regen 2009;17:763–771.

7 Lesher AP, Curry RH, Evans J et al. Effectiveness of Biobrane for treatment of partial-thickness burns in children. J Pediatr Surg 2011;46:1759–1763.

8 Rahmanian-Schwarz A, Beiderwieden A, Willkomm LM et al. A clinical evaluation of Biobrane® and Suprathel® in acute burns and reconstructive surgery. Burns 2011;37:1343–1348.

9 Visconti RP, Kasyanov V, Gentile C et al. Towards organ printing: Engineering an intra-organ branched vascular tree. Expert Opin Biol Ther 2010;10:409–420.

10 Fedorovich NE, Alblas J, de Wijn JR et al. Hydrogels as extracellular matrices for skeletal tissue engineering: State-of-the-art and novel application in organ printing. Tissue Eng 2007; 13:1905–1925.

11 Mironov V, Boland T, Trusk T et al. Organ printing: Computer-aided jet-based 3D tissue engineering. Trends Biotechnol 2003;21:157–161.

12 Maxson S, Lopez EA, Yoo D et al. Concise review: Role of mesenchymal stem cells in wound repair. Stem Cells Translational Medicine 2012;1:142–149.

13 Wang X, Li C, Zheng Y et al. Bone marrow mesenchymal stem cells increase skin regeneration efficiency in skin and soft tissue expansion. Expert Opin Biol Ther 2012;12:1129–1139.

14 De Coppi P, Bartsch G, Jr., Siddiqui MM et al. Isolation of amniotic stem cell lines with potential for therapy. Nat Biotechnol 2007;25: 100–106.

15 Moorefield EC, McKee EE, Solchaga L et al. Cloned, CD117 selected human amniotic fluid stem cells are capable of modulating the immune response. PLoS One 2011;6: e26535.

16 Yoo JJ, Atala A, Binder KW et al. Delivery System. U.S. patent application 20110172611. July 14, 2011.

17 Kolambkar YM, Peister A, Soker S et al. Chondrogenic differentiation of amniotic fluid-derived stem cells. J Mol Histol 2007;38:405–413.

18 Delo DM, De Coppi P, Bartsch G, Jr., et al. Amniotic fluid and placental stem cells. Methods Enzymol 2006;419:426–438.

19 Valli A, Rosner M, Fuchs C et al. Embryoid body formation of human amniotic fluid stem cells depends on mTOR. Oncogene 2010;29: 966–977.

20 Yoon BS, Moon JH, Jun EK et al. Secretory profiles and wound healing effects of human amniotic fluid-derived mesenchymal stem cells. Stem Cells Dev 2010;19:887–902.

21 Mirabella T, Hartinger J, Lorandi C et al. Proangiogenic soluble factors from amniotic fluid stem cells mediate the recruitment of endothelial progenitors in a model of ischemic fasciocutaneous flap. Stem Cells Dev 2012;21: 2179–2188.

22 Mirabella T, Cilli M, Carlone S et al. Amniotic liquid derived stem cells as reservoir of secreted angiogenic factors capable of stimulating neo-arteriogenesis in an ischemic model. Biomaterials 2011;32:3689–3699.

23 Brower J, Blumberg S, Carroll E et al. Mesenchymal stem cell therapy and delivery systems in nonhealing wounds. Adv Skin Wound Care 2011;24:524–532; quiz 533–524.

24 Sorrell JM, Caplan AI. Topical delivery of mesenchymal stem cells and their function in wounds. Stem Cell Res Ther 2010;1:30.

25 Akela A, Nandi SK, Banerjee D et al. Evaluation of autologous bone marrow in wound healing in animal model: A possible application of autologous stem cells. Int Wound J 2012;9:505–516.

26 Rustad KC, Wong VW, Sorkin M et al. Enhancement of mesenchymal stem cell angiogenic capacity and stemness by a biomimetic hydrogel scaffold. Biomaterials 2012;33:80–90.

27 Marga F, Neagu A, Kosztin I et al. Developmental biology and tissue engineering. Birth Defects Res C Embryo Today 2007;81:320–328.

28 Norotte C, Marga FS, Niklason LE et al. Scaffold-free vascular tissue engineering using bioprinting. Biomaterials 2009;30:5910–5917.

29 Skardal A, Zhang J, McCoard L et al. Dynamically crosslinked gold nanoparticle-hyaluronan hydrogels. Adv Mater 2010;22:4736–4740.

30 Skardal A, Zhang J, McCoard L et al. Photocrosslinkable hyaluronan-gelatin hydrogels for two-step bioprinting. Tissue Eng Part A 2010;16:2675–2685.